Wat. Res. Vol. 28, No. 1, pp. 91–106, 1994
Printed in Great Britain.

0043-1354/94 $6.00 + 0.00

SUBMICRON PARTICLES IN THE RHINE RIVER—I. PHYSICO-CHEMICAL CHARACTERIZATION

DIDIER PERRET*, MEREDITH E. NEWMAN, JEAN-CLAUDE NÈGRE, YUWEI CHEN and JACQUES BUFFLE†

Department of Analytical, Inorganic and Applied Chemistry, University of Geneva, 30 Quai Ernest Ansermet, CH-1211 Geneva 4, Switzerland

(First received July 1992; accepted in revised form April 1993)

Abstract—This paper describes a complete sampling, fractionation and characterization scheme for submicrometer particles isolated from the Rhine River. Decreasing particle size fractions were obtained by means of gravitational sedimentation, cascade centrifugation/ultracentrifugation and cascade filtration. These size fractions were analyzed by photon correlation spectroscopy (PCS), micro-electrophoresis (ME), transmission electron microscopy (TEM), light scattering (LS), inductively coupled plasma–atomic emission spectrometry (ICP–AES) and total organic carbon (TOC), which gave complementary results concerning the nature of the particles. The data indicated that submicron particles contribute only a small proportion of the total particle mass and volume, but an important proportion of the total particle number. Moreover, their specific surface area may be quite large. Associations of submicrometer particles with organic macromolecules and fibrils, which may have maintained such particles in suspension, were observed.

Key words—submicron particles, colloids, aggregation, coagulation, inorganic and organic associations, river, sedimentation, centrifugation, filtration, PCS, TEM, TOC, electrophoresis, light scattering

INTRODUCTION

A great deal of evidence indicating that inorganic and organic particles in natural waters play an important role in the circulation processes of nutrients and pollutants has been amassed (Kavanaugh and Leckie, 1980; Anderson and Rubin, 1981; Baccini, 1984; Salomons and Förstner, 1984; Sigg, 1987; Buffle, 1988). However, while particles larger than several micrometers have been extensively studied (Lerman, 1979; Stumm, 1985, 1987), very little is known concerning the physico-chemical characteristics of natural submicron particles, which, due to their high specific surface areas, may play a major role in the control and scavenging of vital and toxic dissolved species.

From data available in the literature (Van de Meent *et al.*, 1983; Nomizu *et al.*, 1987; Rees and Ranville, 1988; Buffle, 1988), it appears that submicron particles in oxygenated waters of rivers and lakes are mainly made of organic matter (fulvics, humics, polysaccharides, proteins), silica, iron oxyhydroxides and possibly small clay particles and that, while representing only a small fraction (< 10%) of the total particle mass, their number increases with decreasing particle size (Buffle and Van Leeuwen, 1992). It is therefore necessary to develop sound schemes for the physico-chemical characterization of these submicron particles, in order to gain information for a better understanding of their behavior in natural waters.

In this article, a sampling, fractionation and analysis scheme developed and applied for the characterization of submicron particles in the Rhine River near Basle (Switzerland) is presented. Other results obtained with this scheme are also presented in the following paper (Newman *et al.*, 1994). The scheme includes sedimentation, centrifugation and filtration as fractionation methods, and photon correlation spectroscopy (PCS), micro-electrophoresis (ME), transmission electron microscopy (TEM), light scattering (LS), inductively coupled plasma–atomic emission spectrometry (ICP–AES) and total organic carbon (TOC) as analytical techniques. It should be emphasized here that fractionation of the raw water is a prerequisite for the accurate characterization of submicron particles, because the obtaining of data on these particles by PCS and TEM is usually hampered, if not completely prevented, by the presence of larger particles. The advantages and limitations of this scheme will also be discussed.

DESCRIPTION OF THE COMPLETE SCHEME

Materials and apparatus

Chemicals used throughout were Merck and Fluka *pro analusis* grade, except for acidification of TOC samples (Merck suprapur). Water used for dilutions and blanks was produced by a Millipore Milli-Q apparatus. Laboratory manipulations were carried out under a class 100 clean bench (ADS Laminaire).

*Present address: Institute of Inorganic and Analytical Chemistry, University of Lausanne, 3 Place du Château, CH-1005 Lausanne, Switzerland.
†Author to whom all correspondence should be addressed.

A high speed pump (Marina Jolly 800; flow-rate > 1 l/s) was used for river sampling. Dissolved oxygen and temperature were measured with an *in situ* probe (Orbisphere Laboratories, Model 2607), and pH was measured with a portable pH-meter (Metrohm E604). Sedimentation was achieved in thermostated sedimentation tanks fabricated for this purpose (Fig. 4).

Suspensions were filtered at 4°C through 0.8 and 0.05 μm pore size polycarbonate membranes (Nucleopore), in filtration cells also fabricated for this purpose. A Heraeus 2.0RS centrifuge with swing-out rotor [maximum radius: 20.7 cm; maximum speed: 4000 rpm (3700 *g*); polycarbonate tubes] was used for field centrifugations, and a Beckman L7-55 ultracentrifuge with swing-out rotor SW30 [maximum radius: 12.5 cm; maximum speed: 30,000 rpm (124,000 *g*); polyallomer and polycarbonate tubes] was used for laboratory centrifugations.

Field and laboratory LS measurements were made with a Merck–Hitachi F-1050 flow-through fluorimeter (excitation and emission monochromators set to zero order).

PCS and ME measurements were made using a Malvern Zeta Sizer III photon correlation spectrometer equipped with a 256 channel correlator and a 1W Ar laser (Coherent Innova 70; 488 nm wavelength); focusing lenses were added to the instrument in order to improve the detection limit.

Electron microscopy observations were made using a medium resolution TEM (Zeiss EM-109), a high resolution TEM (Philips EM300) and a SEM (JEOL JSM6400). For TEM, specimens were deposited on 200 mesh Cu grids (Embra), and protected with a hydrophilic resin (Nanoplast).

A Dohrman DC80 instrument with a u.v. reactor and a linearized non-dispersive i.r. detector was used for TOC measurements.

ICP–AES of sonicated (Branson 250) suspensions were made using a Perkin–Elmer Plasma 1000 spectrometer (λ_{Ca}: 393.366 nm; λ_{Mg}: 279.553 nm; λ_{Al}: 396.152 nm; λ_{Si}: 251.611 nm; λ_{Fe}: 238.204 nm; λ_{Mn}: 257.610 nm; Ar flow-rate: 15 ml/min).

The complete sampling, fractionation and characterization scheme for submicron particles applied to the Rhine River during 1990–1991 is schematized in Fig. 1 and is discussed in detail below.

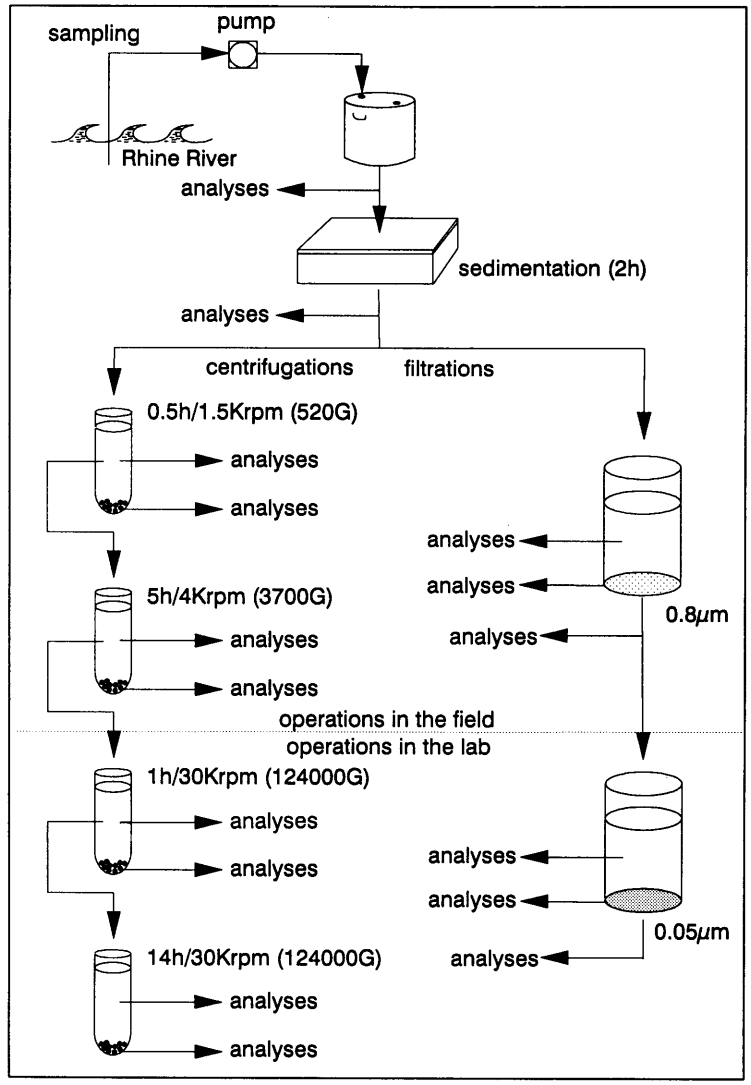

Fig. 1. Sampling, fractionation and analysis scheme for particulate samples in the Rhine River; operations were made directly in the field (upper part of the figure), then in the lab (lower part); centrifugations and filtrations were started and pursued in parallel.

Storage conditions

In order to avoid contamination, closed polycarbonate and polyethylene containers were presoaked with 1 M HNO_3, rinsed with filtered Millipore Milli-Q water and ethanol, dried and then stored in a clean bench prior to use. Samples were processed as soon as possible for PCS and TEM analyses (less than 6 h between recovery of a fraction and TEM specimen preparation); they were stored at 4°C before ICP–AES and TOC analyses.

Initial tests were made in order to assess the efficiency of sodium hexametaphosphate (HMP) as an anticoagulant (Gallegos and Menzel, 1987), and mercuric chloride or sodium azide as antibiotics (Burdon and Williams, 1969; Fox, 1988). The results of these tests showed that:

(1) HMP, when used at 0.1–1%, may decrease LS intensities of raw and sedimented samples, because of the disaggregation of previously coagulated particles; this hypothesis was confirmed by PCS observations. After a storage time of 2–3 days, however, HMP may enhance coagulation (Fig. 2), by an increase in ionic strength (coagulation promoted by Na^+) or by the hydrolysis of HMP into orthophosphates followed by precipitation of $Ca_3(PO_4)_2$ (samples being stored at 4°C).

(2) $HgCl_2$ ($0.4–4 \times 10^{-4}$ M) or NaN_3 ($10^{-4}–1.5 \times 10^{-2}$ M) were both tested as antibiotics. However, they did not decrease bacterial growth in samples stored at 4°C for more than 5–7 days. Higher concentrations could not be used, since Hg(II) precipitated as hydroxide, while NaN_3 interfered with TOC analyses.

(3) Both PCS and TEM analyses indicated that storage of water samples at 4°C in darkness without the addition of either an anticoagulant or an antibiotic was possible for periods of up to 4 days, without any obvious change in size distribution, morphology of particles, or bacteria concentration, provided the storage vessels were washed with ethanol before introducing the sample.

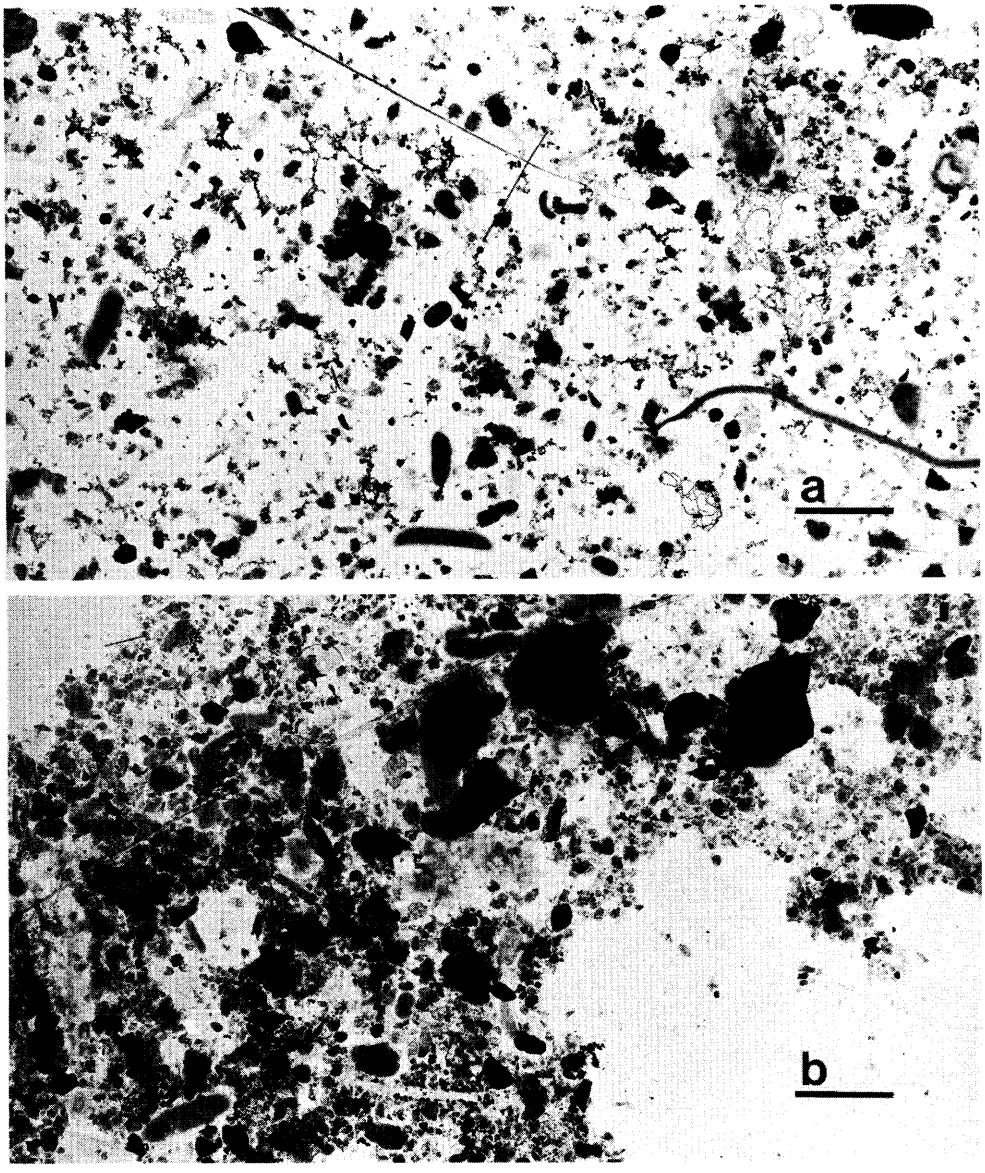

Fig. 2. TEM images of (a) a sample stored 2 days at 4°C without preservative and (b) the same sample stored 2 days at 4°C with HMP added (1%). Sampling date: 12 March 1991. Bar = 2 μm.

Systematic tests are needed in order to determine the precise role of HMP in both disaggregation and aggregation processes, and the most appropriate concentrations of antibiotics. However, in view of observation (3), we chose not to use foreign compounds for sample preservation. Instead, all fractionation steps (Fig. 1), PCS measurements and TEM grid preparations were completed within a maximum of 4 days after collection to avoid contamination and modification of samples. In most cases, centrifugations, PCS and TEM preparations were completed within 48 h. This procedure eliminated many artifacts commonly encountered with particulate samples stored longer than 4 days.

Sampling and sedimentation

Rhine River water was sampled from a boat at Birsfelden (Basle, Switzerland), at a single point located between a hydroelectric power plant and the input of the Birse River (Fig. 3), using a high speed pump at 1 m below surface level. No visual aggregation was observed after collection, as is the case for estuarine waters. During transportation to the shore, raw water was stored in 30 l. polyethylene reservoirs.

Immediately after returning to shore, sedimentation tanks fabricated for this purpose (Fig. 4) were filled with raw water (*c.* 27 l) which was allowed to settle under quiescent conditions for 2 h (see below). This preliminary sedimentation step was carried out in order to remove large/dense particles which might interfere with the subsequent analysis steps. The time interval between sampling and beginning sedimentation was less than 30 min; the sedimentation tanks were preconditioned for 12 h with river water which was removed immediately before use.

At the end of this sedimentation step, the supernatant was recovered by pumping out the water layer between 1.5 and 2 cm (sampled volume: 1200 ml) below the surface level, through an 8-fold tubing assembly uniformly arrayed on the lid of the tank and connected to a low flow-rate (200 ml/min) peristaltic pump. This supernatant was used within less than 15 min for the subsequent factionation steps (see following two sections).

A sedimentation time of 2 h and a sampling depth between 1.5 and 2 cm have been selected for the following reasons:

(1) The top 1.5 cm water layer was not sampled in order to avoid the recovery of floating organic debris. Indeed, during preliminary tests, light scattering intensity versus sedimentation time was higher when the solution was pumped out of the tank from the surface water layer than when sampled from 1.5 cm below the surface. Temperature control of the sedimentation tank has been found to be essential; in particular, when water is colder than the atmosphere, warming of the sample during sedimentation forms microbubbles on the colloidal particles which subsequently accumulate at the air–water interface by flotation.

(2) The sedimentation rate of a particle depends on its size and density. Table 1 gives representative size fractionation values based on Stokes law [$v_{sed} = d^2(\rho - \rho_s)\,g/18\eta$ (cm/s), where d = diameter of spherical particle (cm), ρ, ρ_s = density of particle and solution (g/cm^3), η = viscosity of solution (g/cm · s), g = gravity (cm/s^2)], for different scenarios of particle size and density. It can be seen from this that large or dense particles ($d \geqslant 2\ \mu$m for $\rho \approx 3$ g/cm^3, representative of inorganic material, to $d \geqslant 9\ \mu$m for $\rho \approx 1.1$ g/cm^3, representative of organic material) are removed from the top 2 cm of the suspension within 2 h.

(3) Irrespective of the hydraulic loading of the river, plots of light scattering intensity versus sedimentation time (Fig. 5) showed the scattering intensity to decrease to a relatively constant value within 2 h. Therefore, a 2 h sedimentation time was selected for subsequent fractionations.

Centrifugation and ultracentrifugation

Fractionation by filtration has been used more frequently in the past than sedimentation and centrifugation, especially for field studies. However, these various techniques offer different advantages and disadvantages. Filtration tends to coagulate particles at the surface of membranes when used under uncontrolled conditions (high flow-rate, no stirring, large filtered volume; Buffle *et al.*, 1992). Centrifugation is less sensitive to fractionation conditions than filtration, although it has been suggested that it may produce aggregates (Salim and Cooksey, 1981). Unlike filtration, neither centrifugation nor gravitational sedimentation allow direct size fractionation, but rather isolation of particles with

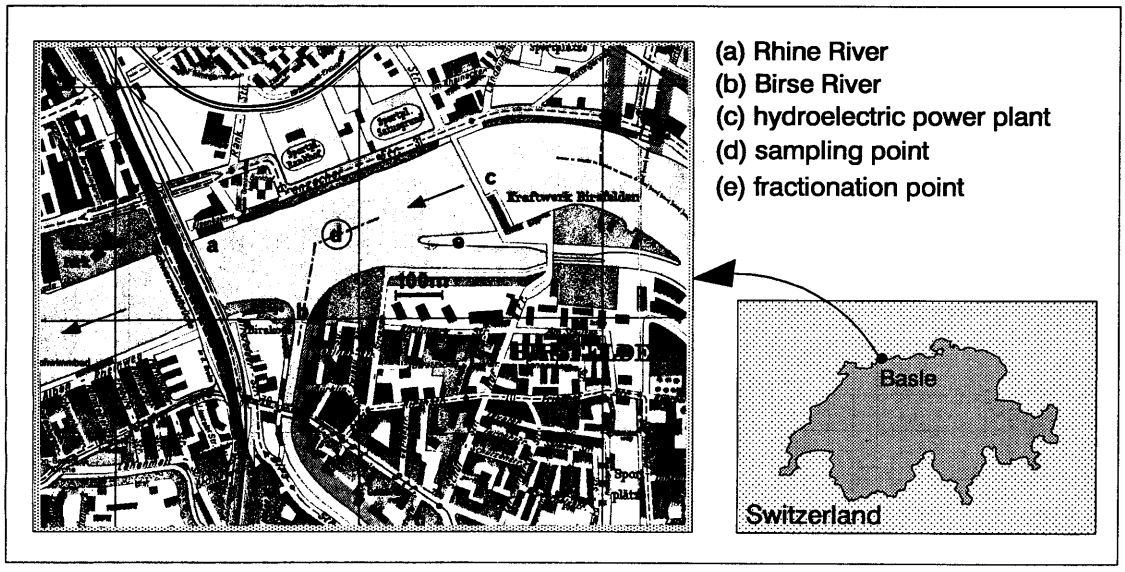

Fig. 3. Sampling location in Basle (Switzerland); the Rhine River was sampled 1 m below the surface, at a point located between the hydroelectric power plant (Birsfelden) and the input of the Birse River.

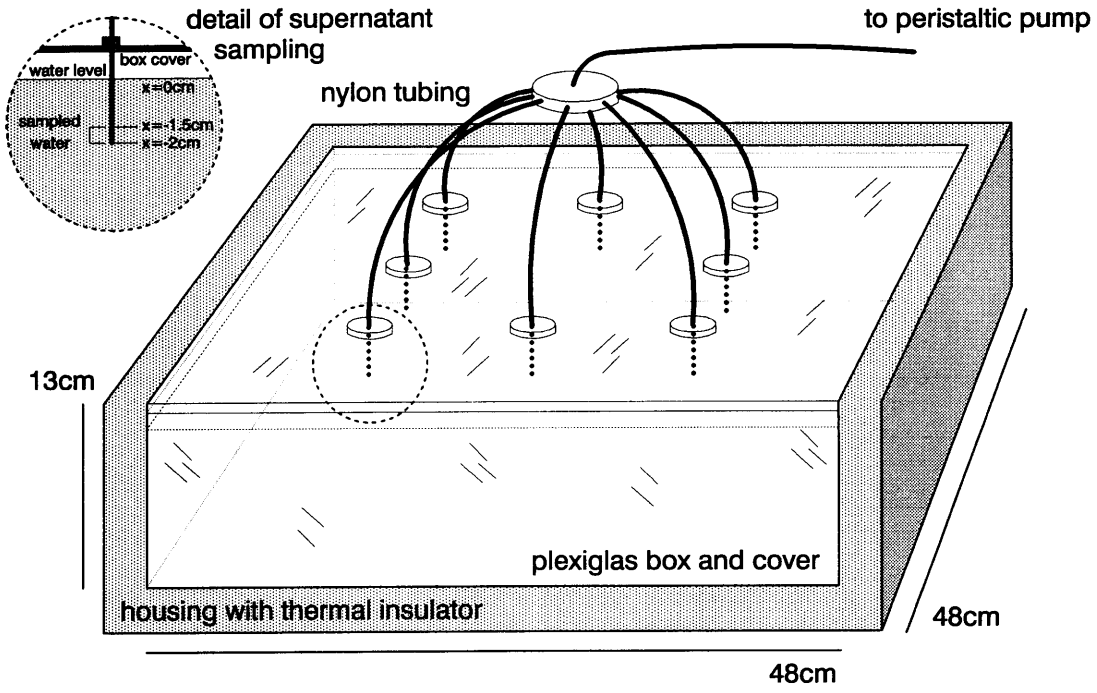

Fig. 4. Sedimentation tank used for the elimination of large and dense particles. In order not to create turbulences in the supernatant layer, the tubing assembly was connected to a slow flow-rate peristaltic pump for sampling.

similar composite characteristics (size and density). Because of their complementarity, centrifugation and filtration were used in parallel for the Rhine River studies for comparative purposes (Fig. 1).

Centrifugations were performed in cascade, i.e. the supernatant of the first centrifugation was used in the second centrifugation, etc. This procedure assured that the largest and densest particles were removed during the first centrifugation and were not present in subsequent steps. Coagulation artifacts caused by differential settling (coagulation between large rapidly sedimenting particles and small slowly sedimenting ones) were thus minimized by this procedure. Supernatants of centrifugations were recovered with a low flow-rate (50 ml/min) peristaltic pump in order to prevent perturbation of the pellets.

The centrifugation conditions (Table 1; Fig. 1) were selected in order to obtain colloidal fractions as different as possible from each other, and taking into account the characteristics of the centrifuges, the volumes necessary for analyses, and the amount of time available in the field. All centrifugations were carried out at 5°C. Estimations of particle size ranges for the various fractions, as calculated by Stokes law, are given in Table 1. The conditions of centrifugation steps were the following:

Step 1: 0.5 h at 1500 rpm (520 g; centrifugation of sedimented solution in the field). A volume of 1040 ml was centrifuged (V_{in}), and 640 ml (160 ml for analyses, 480 ml for step 2) were recovered (V_{out}).
Step 2: 5 h at 4000 rpm (3700 g; centrifugation of supernatant from step 1 in the field). $V_{in} = 480$ ml, $V_{out} = 280$ ml (160 ml for analyses, 120 ml for step 3). The time interval between the end of step 2 and the beginning of step 3 was less than 4 h.
Step 3: 1 h at 30,000 rpm (124,000 g; ultracentrifugation of supernatant from step 2 in the lab). $V_{in} = V_{out} = 120$ ml (20 ml for analyses, 100 ml for step 4).
Step 4: 14 h at 30,000 rpm (124,000 g; ultracentrifugation of supernatant from step 3 in the lab). $V_{in} = V_{out} = 100$ ml (for analyses).

The fractionation scheme described above allowed fractionation of particles in the range from a few nanometers to a few microns within approx. 24 h (including transportation from field to lab).

Filtration

Filtration has been extensively applied as a fractionation technique in field studies (Buffle *et al.*, 1992). One of the

Table 1. Minimum diameter [d (μm)] of particles with different densities [ρ (g/cm^3)] eliminated during sedimentation or centrifugation at 4°C, as calculated by Stokes law. For sedimentation, particles have to sediment through a 2 cm layer in the tank for 2 h. For centrifugation, calculations integrate the increasing centrifugal field applied on particles when they sediment in the tube

	Minimum diameter of particles eliminated by gravitational sedimentation and centrifugation			
	$\rho = 1.1$(g/cm^3)	$\rho = 1.5$(g/cm^3)	$\rho = 2.0$(g/cm^3)	$\rho = 3.0$(g/cm^3)
Sedimentation $V_{sed} = 1$(cm/h)	>9 μm	>4 μm	>3 μm	>2 μm
Centrifugation step 1: 0.5 h; 1500 rpm	>2 μm	>900 nm	>600 nm	>450 nm
Centrifugation step 2: 5 h; 4000 rpm	>230 nm	>110 nm	>75 nm	>50 nm
Centrifugation step 3: 1 h; 30,000 rpm	>65 nm	>30 nm	>20 nm	>13 nm
Centrifugation step 4: 14 h; 30,000 rpm	>20 nm	>8 nm	>6 nm	>3.5 nm

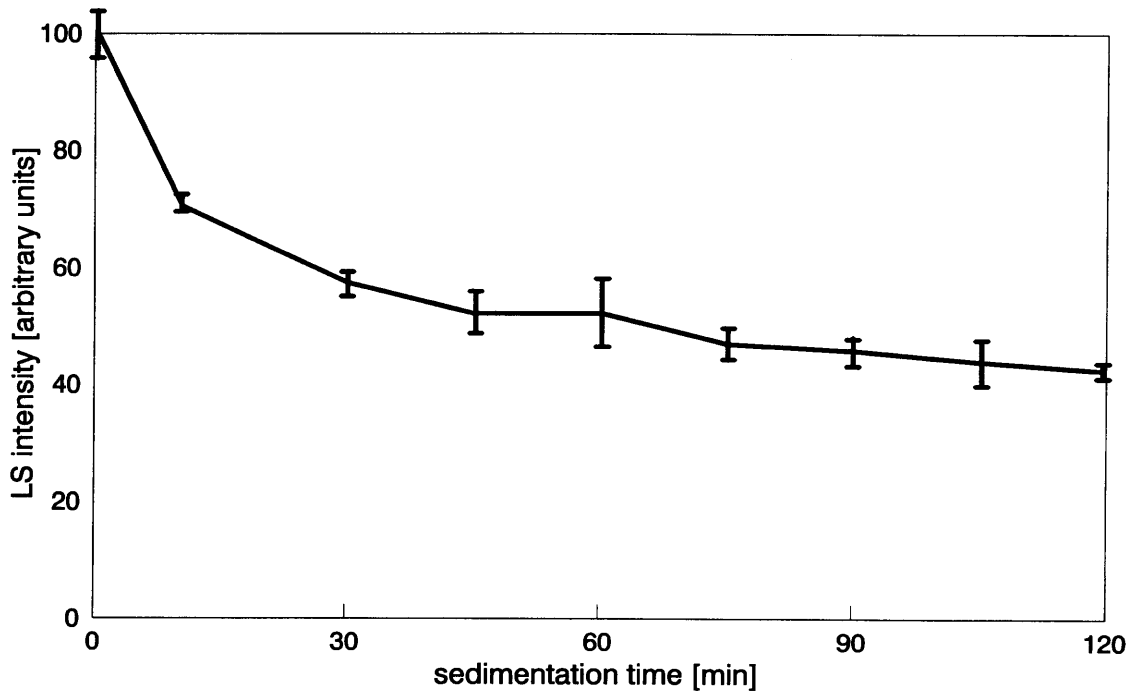

Fig. 5. Typical sedimentation curve obtained by light scattering measurements of aliquots sampled from the sedimentation tank; samples were directly injected into the fluorimeter set to zero order. Sampling date: 13 August 1991.

main drawbacks of filtration (i.e. the creation of artifacts caused by coagulation of colloids at the membrane surface) can be minimized by using small concentration factors (i.e. low ratio of volume introduced in the cell to volume remaining in the cell at the end of the filtration) and very low flow-rates (typically $< 10^{-4}$ cm s^{-1}; Buffle *et al.*, 1992). Cascade filtrations (where the filtrate from the previous filtration is subsequently introduced into the following filtration cell which contains a lower porosity membrane) have been used under carefully controlled conditions in this investigation. Samples were filtered without stirring at 4°C under helium pressure; helium was used instead of N_2 because of its lower solubility in water, in order to avoid bubble formation at the outlet of the filtration cells which were connected on-line to a light-scattering spectrometer; N_2 gas bubbles interfered with measurements. The following filtration conditions were chosen (Fig. 1):

- Step 1 consisted of filtering the sedimented sample through a 0.8 μm pore size Nuclepore membrane (polycarbonate; diameter: 90 mm), at 3×10^{-5} cm/s flow-rate (0.5 ml/min), with a concentration factor of 3.6, in the field. Two identical filtrations were carried out in parallel. The volume introduced into each cell (V_{in}) was 430 ml.
- Step 2 consisted of filtering the 0.8 μm filtrate through a 0.05 μm pore size Nuclepore membrane (polycarbonate; diameter: 90 mm), at 3×10^{-5} cm/s flow-rate (0.5 ml/min), with a concentration factor of 2.4, in the lab. Only one filtration was carried out, due to limitations of sample volume and time. V_{in}: 450 ml.

Filtration membranes were checked for tears, altered pore size and clogging, by scanning electron microscopy (SEM) analyses. Irreproducible results were obtained for preliminary tests with Amicon PM10 membranes (*c.* 2 nm pore size), which were thus abandoned.

Direct filtrations of raw and sedimented samples through preweighed 0.1 μm pore size Nuclepore membranes (polycarbonate) were also systematically performed in order to determine the total mass of particles in these two fractions. The mass concentration of particles in the samples was determined by weighing the dried membranes after filtration. High flow-rate and filtration to dryness were used in this case to enhance membrane clogging and improve the recovery of particles smaller than the pore size of the membranes.

Photon correlation spectroscopy

Photon correlation spectroscopy (PCS) yields a weighted average size distribution of the sample, contrarily to TEM which allows determination of single particle sizes. PCS is based on the instantaneous changes in light scattering caused by the Brownian motion of submicron particles. The theory and design of PCS systems as well as their application to environmental samples have been reviewed elsewhere (Ford, 1983; Schurtenberger and Newman, 1994). Light scattering sensitivity depends on particle size; for an Ar laser ($\lambda = 488$ nm) and an angle of 90°, light scattering is optimal for approx. 100 nm particles, and decreases significantly for smaller particles (Newman and Buffle, 1994). Samples must then be fractionated prior to PCS analysis, since large particles (> 100 nm) scatter light more effectively than small ones (< 100 nm), and may mask their presence in the sample.

PCS analyses reported here were carried out at least at three scattering angles in order (i) to check for masking of small particles by the greater scattering intensities of the larger particles and (ii) to verify that particles of all sizes present were identified. Angles for analyses were selected after first scanning the light scattering intensity for each angle from 45 to 120°. Details concerning practical problems and choice of optimum operating conditions are described elsewhere (Newman and Buffle, 1994).

The mean and standard deviation values reported for PCS analyses represent a minimum of three, and frequently as many as 15, replicates. These include analyses made at

varying scattering angles. The corresponding variability of scattered light is estimated to be 10–15% for fractionated samples, while the variability associated with measurements of raw and sedimented samples is much greater and is difficult to quantify.

Mie theory was used to calculate the mass or volume weighted size distribution from the scattering intensity weighted distributions; knowledge of the particle refractive index was required for these calculations (Ford, 1983; Newman and Buffle, 1994). TEM observations indicated the greatest proportion of particles present in the Rhine samples were clays. Therefore a refractive index of 1.6, typical of values commonly measured for clays, was used to obtain the mass and volume distributions reported here.

Assuming the refractive index of the particles in the river did not vary by more than 10% from the value of 1.6 selected, the error associated with the mass and volume distributions calculated for the fractionated samples was again approx. 10–15%. However, since the particle number weighted distributions depend on the sixth power of the measured light scattering intensity, the variability associated with number weighted size distributions is much larger; it is estimated to be as high as 50%.

Micro-electrophoresis

Micro-electrophoresis (ME) was also performed to obtain information on the particle surface charge. The theory and operation of this instrument is essentially the same as for traditional electrophoresis (Harfield and Bunker, 1988; Gaigalas *et al.*, 1990). A voltage is applied across the cell and the direction and velocity of particle motion are measured. Two laser beams intersect and produce interference fringes in the stationary layer of the cell, where the particles move with a velocity which is due solely to their own charge, and is not influenced by the electroosmosis of the fluid. Particles interact with these fringes to produce scattered light which oscillates in time in a way which depends on the velocity of the particles.

The measured autocorrelation function is first converted, using a Fourier Transform, into a frequency spectrum. The frequencies are then converted successively to velocity and electrophoretic mobility. Conversion from electrophoretic mobility ($u[(\mu m/s) \cdot (V/cm)]$) to zeta potential [$\zeta$(mV)] is made using the Smoluchowski equation [$\zeta = u \cdot \eta/\epsilon$, where η = solution viscosity (g/cm · s), and ϵ = dielectric constant], applicable for particles larger than approx. 20 nm in dilute electrolyte solutions ($I < 0.01$ M).

Practically, only average values of electrophoretic mobility and zeta potential, rather than distributions of surface charge, could be obtained by this method. Formation of bubbles in the solution during ME analysis was a frequent problem. The error associated with mean mobility values was approx. 15–20% for each individual sampling date.

Transmission electron microscopy

The use of transmission electron microscopy (TEM) for determining the size, morphology, associations and composition (when used with a specific probe) of submicron particles is well documented (Perret *et al.*, 1991, and references therein; Wells and Goldberg, 1991; Leppard, 1992).

This technique, in conjunction with non-perturbing methods of specimen preparation, allows observation of fine structures at the near nanometer level, unobtainable by SEM. Furthermore, TEM of optimally prepared specimens allows direct visualization of associations between particles, thus providing a method for studying coagulation processes at a qualitative level.

Specimen preparation for TEM analyses of Rhine River samples is described in detail elsewhere (Perret *et al.*, 1991). Raw water, sedimented water, supernatants from cascade centrifugations, and samples from cascade filtrations (filtrates, retentates) were ultracentrifuged at 124,000 *g* (30,000 rpm) for 14 h over TEM grids placed at the bottom of polycarbonate tubes; the volume to be centrifuged in order to obtain optimally dispersed specimens was estimated from LS measurements.

After this ultracentrifugation step, grids were recovered, and divided into two subsets: the first was directly stored for TEM analyses, and the second was protected with Nanoplast, a water-soluble embedding resin (Frösch and Westphal, 1989); grids were placed on top of a horizontal disk, covered with a minute amount of Nanoplast mixture, centrifuged for 30 s and then cured and polymerized (Perret *et al.*, 1991).

While no important differences between uncovered grids and grids protected with Nanoplast were observed by medium resolution TEM, grids protected with Nanoplast, while more frequently damaged (fewer available surfaces for analyses), were better suited for high resolution TEM. In particular, the protective Nanoplast film seems to eliminate shrinkage of particles caused by slow dehydration, and to retain fine organic structures in their original shape, allowing the study of organic/inorganic aggregates at high resolution.

Light scattering

Light scattering (LS) measurements yielded relative estimates of the total particulate content of suspensions. LS is a function of both particle size and concentration; for this reason, LS could not be used as an accurate measure of particulate concentration when the size of particles in fractionated samples was decreasing. However, LS measurements could be made directly in the field, by the use of a flow-through fluorimeter with excitation and emission monochromators set to zero order.

Field and lab measurements were made using the flow-through fluorimeter. Tests with standard solutions of latex and hematite particles showed that the LS analysis of particulate samples gave a reasonable estimate of the relative content of particles in each sample; the variability of LS measurements was estimated to be approx. 10%. For standard measurements, solutions were injected in the flow-through cell with a plastic syringe, at a constant flow-rate (10 ml/min); the complete circuit was purged between samples with filtered Millipore Milli-Q water in order to avoid contamination. For measurements of filtrates, the instrument was directly connected to the outlet of the filtration cells; this procedure allowed real time monitoring of filtration conditions and events. To avoid formation of bubbles in the LS cell, filtrations were achieved under He pressure.

Inductively coupled plasma–atomic emission spectrometry

ICP–AES was used for the determination of the average elemental composition of submicron particles. Ca, Mg, Al, Si, Fe and Mn concentrations were measured.

Particulate matter was isolated from the raw sample and each fraction by ultracentrifugation at 124,000 *g* during 14 h [same conditions as for step 4 centrifugation (Table 1) or TEM specimen preparation]. At the end of the centrifugation step, the supernatant was carefully suctioned off with a peristaltic pump (50 ml/min), and a small volume of 5% HNO_3 was added to the remaining pellet. The resulting suspension was sonicated for 2 min in order to detach any remaining particles from the centrifugation tube, and then analyzed by ICP–AES with a Perkin–Elmer Plasma 1000 spectrometer.

The precision of the particulate Ca and Mg determination was hampered by the high concentrations of these major ions (1.4×10^{-3} M for Ca^{2+}, 3×10^{-4} M for Mg^{+2}) in the dissolved state (see Table 2 for an overview of relevant species). For instance, for an initial solution containing 1 mg/l of particulate $CaCO_3$, 10 μl of centrifuged solution remaining in the tube after supernatant removal causes an error of *c.* 15% in particulate Ca due to the dissolved Ca.

Table 2. Average concentrations of total and dissolved species in the Rhine River (Village Neuf, 8.5 km downstream from Birsfelden), according to EAWAG (1989)

	Ca_{tot}	Mg_{tot}	TOC	DOC	Na	K	Cl	SO_4	P_{tot}	o-PO_4	N_{tot}	NO_3
Concentration (mg/l)	55 ±9	6.8 ±1	3.4 ±1.5	2 ±0.5	8.5 ±4.2	1.7 ±0.4	11.7 ±5.6	28 ±5.5	0.095 ±0.07	0.044 ±0.037	2.4 ±1.4	1.8 ±1.2

In most cases the colloidal concentrations of elements other than Ca and Mg in fractionated samples were initially less than *c.* 30 μg/l (Fig. 6). Although our centrifugal recovery procedure allowed preconcentration of colloids by a factor of 5–10 before ICP–AES analyses, the concentration remained low. As a consequence, the analytical precision for these samples was also low. For raw and sedimented water samples, the particle content was larger; however, they contained a significant fraction of particles larger than 1 μm. Due to extremely high excitation temperatures, Inductively coupled plasma–atomic emission spectrometry (ICP–AES) is better suited for the determination of the elemental composition of natural aquatic particles than other atomic methods (atomic absorption spectrometry, flame emission spectrometry) (Cresser *et al.*, 1990). However, even at torch temperatures exceeding 8000°C, particles larger than a few micrometers are not quantitatively atomized (Foulkes *et al.*, 1988). Thus, it is likely that the results reported for raw and sedimented water are underestimated.

Because of the problems described above, the average variability of ICP–AES measurements was close to 25%. Nevertheless, these results were useful in estimating the evolution of particle composition during the fractionation steps (Fig. 6), and in following relative changes in particle composition with season.

Total organic carbon

TOC measurements were made on samples acidified in the field immediately after collection, and stored in precleaned glass bottles in order to avoid organic contamination by plastic containers.

Figure 7(a) shows typical values of TOC in the raw and sedimented waters, and in the filtrates of 0.8 and 0.05 μm pore size membranes, for normal low conditions. It can be seen that most of the TOC in the raw water is composed of organic compounds smaller than 0.05 μm, which agrees with results reported for pedogenic organic matter in continental surface waters (Buffle, 1988).

Due to the very small differences in TOC between the fractions, and to its rather low value in the raw water, even very small contamination problems made the comparison of TOC values between the various fractions difficult. In particular, it was observed that contact with the plastic centrifugation tubes may have contaminated the samples by 0.2–1.0 mg/l. Therefore, centrifuged fractions were not used to study TOC distributions. Most of the filtration apparatus was composed of nylon tubing and Plexiglas. Previous experiments showed that contamination by these two plastics was minimal. The most important contamination problem in filtration probably arose from the membrane itself. The filtration apparatus was thoroughly washed before use by filtering pure bidistilled or Milli-Q water.

Figure 7(b) shows that, for an 0.8 μm pore size membrane, a washing volume of at least 15 ml/cm^2 was necessary (*c.* 1000 ml for a membrane with a diameter of 90 mm) before use to get a relatively low baseline in LS intensity of the filtrate. Note that even after, the filtrate remained contaminated by 0.2 mg/l of TOC. The values reported for the filtrates of 0.8 and 0.05 μm membranes have been corrected for these residual contaminations. In

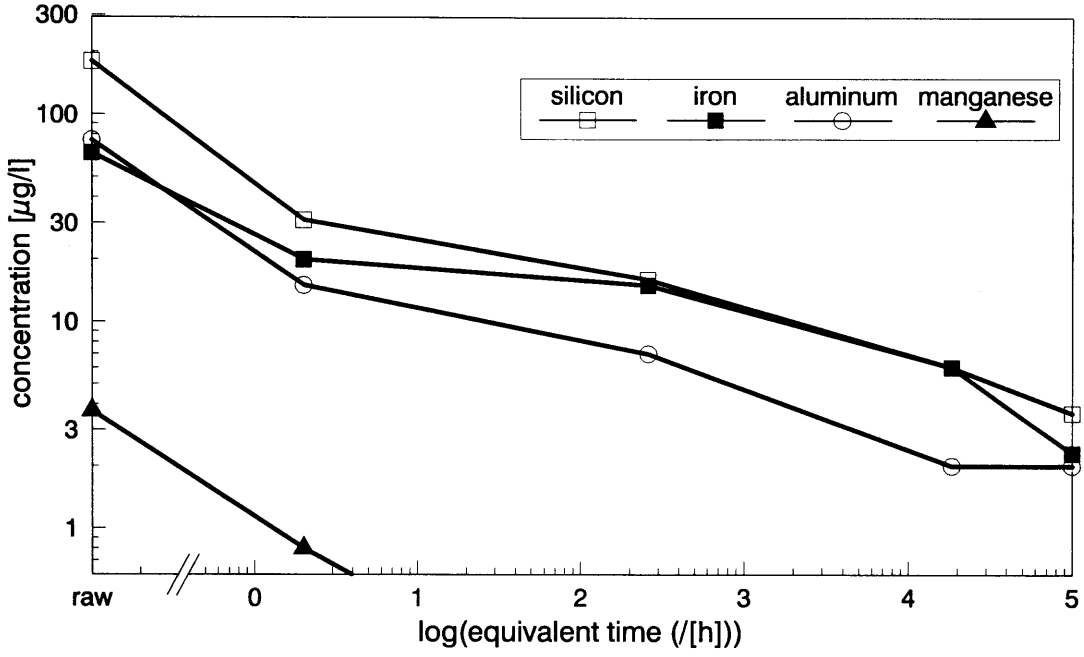

Fig. 6. ICP–AES results, expressed as elemental composition of particles versus fractionation steps; the increasing sedimentation/centrifugation times correspond to decreasing particle sizes (see also Table 1 and Fig. 10). Centrifugation times have been converted to equivalent sedimentation times at 1 *g*. Sampling date: 12 March 1991.

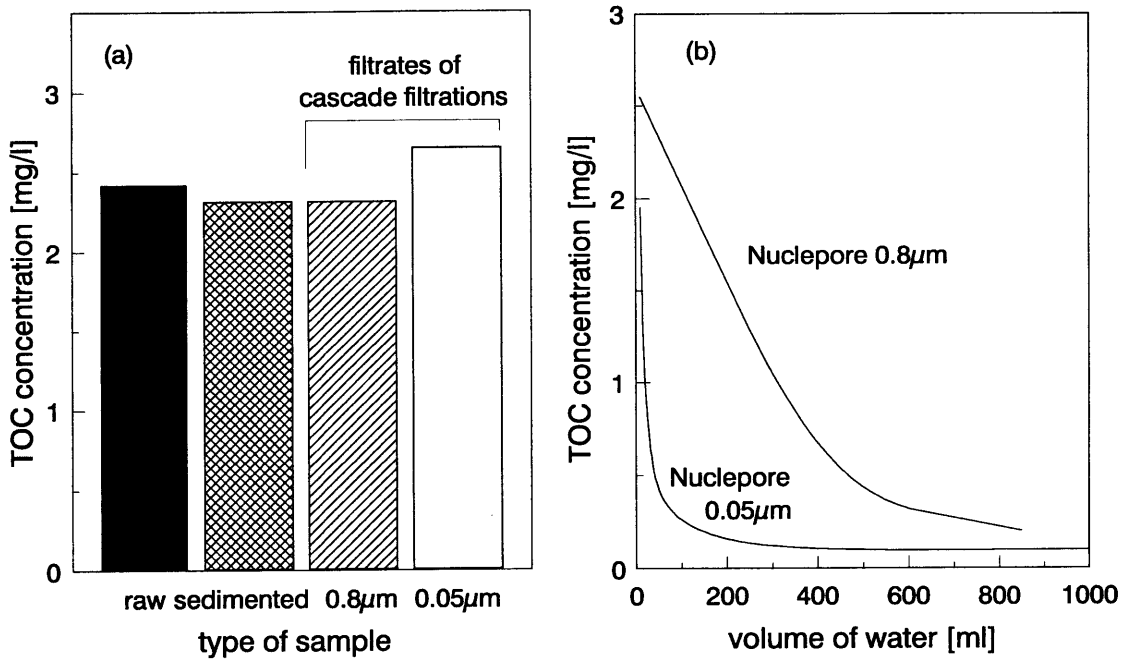

Fig. 7. (a) TOC analyses of raw and sedimented waters, and filtrates of 0.8 and 0.05 μm pore size membranes. Sampling date: 22 October 1991. (b) TOC values of filtrates obtained during the washing of unused Nuclepore membranes with Millipore Milli-Q water.

Fig. 7(a), the larger TOC value obtained for the 0.05 μm filtrate is due to non-corrected contaminations.

RESULTS AND DISCUSSION

Global characteristics of particles

Typical elemental concentrations of Si, Al, Fe and Mn, in the various fractions are shown in Fig. 6. Additional results are presented in Newman *et al.* (1994). Calcite-type particles (mainly > 1 μm) were systematically identified by ICP–AES and TEM observations in raw and sedimented samples, but less frequently observed (5–10 times less, or even lower) in filtrates and supernatants of centrifugations. Magnesium, silicon, aluminum and iron showed similar trends. TEM observations indicated that these elements were primarily present as diatom fragments (sizes of fragments *c.* 0.1–1 μm), clays (different morphologies, with a large size distribution, *c.* 50 nm to several microns), and iron and silica particles (near spherical shapes, high electron density, sizes <0.5 μm).

The fairly constant organic matter concentration, close to 2.5 mg/l in the various fractions, suggests that the majority of organic material was present in solution as very small, low density, colloidal particles. This observation was confirmed by TEM analyses: a few large pieces of organic debris (algae fragments and cells, with sizes ranging from 0.5 to 5 μm) and bacteria (having a relatively constant size, close to 1 μm) were seen in the raw and sedimented fractions; but when large particles, which could interfere with observations, were eliminated (as in centrifuged or filtered fractions), many weakly electron dense objects of organic origin with sizes usually much smaller than 0.5 μm were observed (Fig. 8).

Size distribution and inorganic/organic associations

PCS analyses over the entire year showed the existence of three major particle size classes: (i) larger than 1 μm, (ii) comprised between 0.2 and 0.7 μm and (iii) smaller than 0.2 μm (Fig. 9). Particles larger than 1 μm may be further divided into classes comprised between 1 and 3 μm and larger than 3 μm [see Newman *et al.* (1994) for details]. These results show that particles smaller than 0.2 μm contribute a negligible proportion (less than 2%) of the total particle volume and mass. However, as discussed later, they may represent a dominant proportion of the available surface area for adsorption of pollutants.

Figure 10 shows typical PCS size distributions for the various size fractions obtained by sedimentation and centrifugation. Similar distributions were observed throughout the year.

As mentioned before, the largest particles (size > 1 μm) contributed the majority of the total mass, while the smallest particles (0.05–0.2 μm) are present in the greatest number. Another important result shown in Fig. 10 is that particles of 200–300 nm remained in solution even after centrifugation for 5 h at 3700 ***g*** (which corresponds to centrifugation step 2 in Fig. 1). In order for particles of 200–300 nm to remain suspended under these conditions, they must be largely organic ($\rho \approx 1.1$ g/cm^3; Table 1).

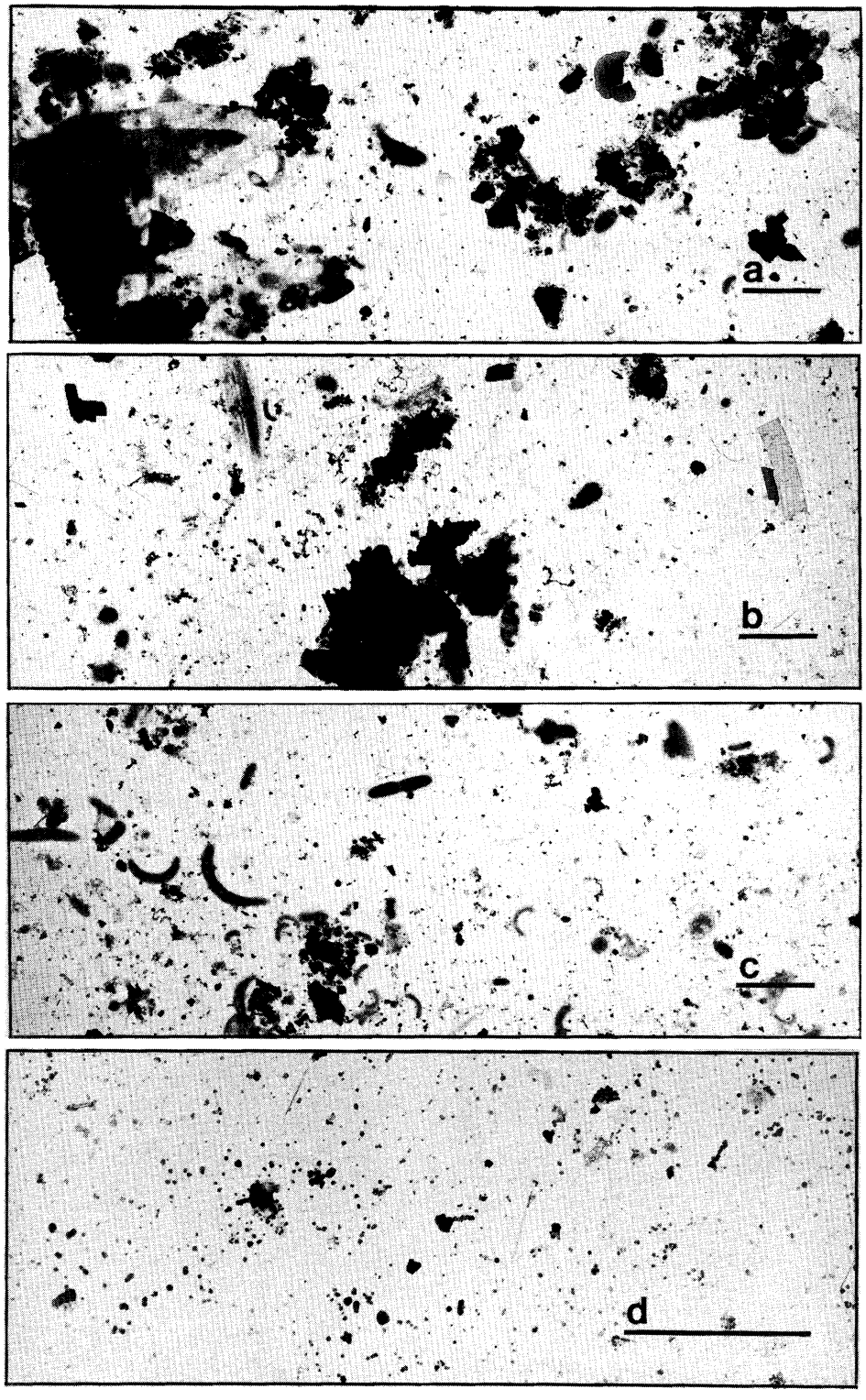

Fig. 8(a)–(d). *Caption opposite.*

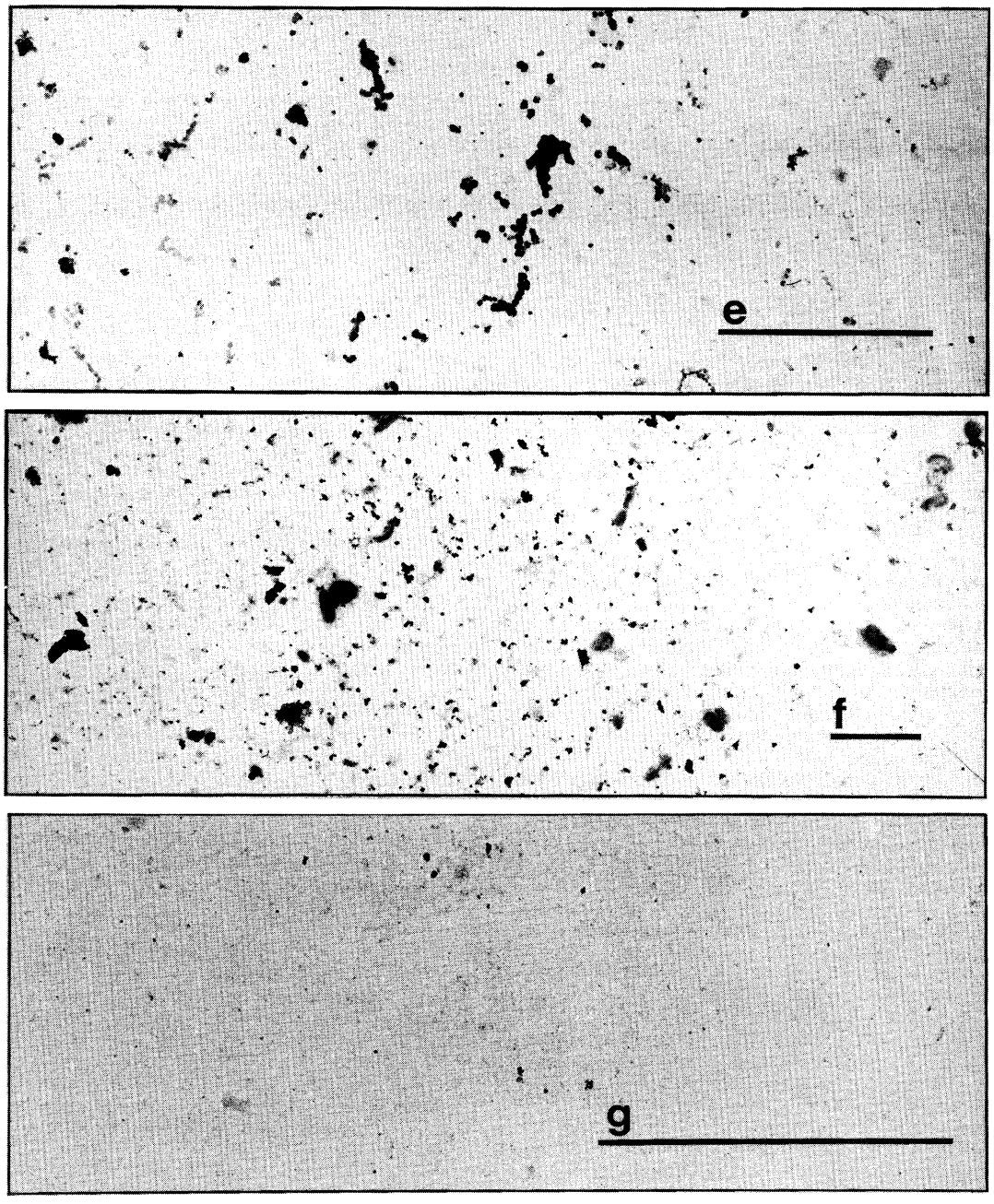

Fig. 8(e)–(g)

Fig. 8. Typical TEM pictures of (a) raw Rhine River, (b) sedimented sample (2 h sedimentation), (c) supernatant of centrifugation step 1 (0.5 h, 1500 rpm), (d) supernatant of centrifugation step 2 (5 h, 4000 rpm), (e) supernatant of centrifugation step 3 (1 h, 30,000 rpm), (f) filtrate of filtration step 1 (0.8 μm pore size) and (g) filtrate of filtration step 2 (0.05 μm pore size). Sampling date: 13 August 1991. Bar = 2 μm.

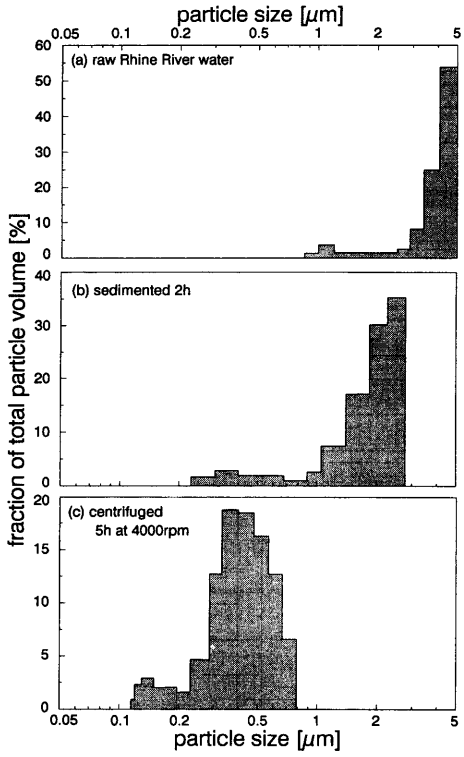

Fig. 9. Typical volume weighed particle size distributions obtained (a) on raw water, (b) after sedimentation of raw water and (c) after centrifugation of sedimented water, showing the shift in size towards smaller particles after fractionation. Sampling date: 13 August 1991. The upper size limit is imposed by the PCS instrument, and the size distribution in (a) should only be taken as an indicative view of the true distribution.

Electrophoretic mobilities were measured for three sampling dates (18 June 1991, 13 August 1991, 22 October 1991). For these three dates, mean values of electrophoretic mobilities of -1.48 (± 0.97) and -1.40 (± 0.71)(μm/s)$\cdot$(V/cm), corresponding to mean zeta potentials of -21.8 (± 13.1) and -17.6 (± 6.9) mV have been obtained for sedimented samples, and mixed fractions of centrifugation steps 1 and 2, respectively. The values observed are within the range of values reported in the literature for similar natural particles (Bryant and Williams, 1987; Rees and Ranville, 1990), and correspond to the slightly negative electrophoretic mobilities observed for natural particles with organic surface coatings (Tipping and Higgins, 1982).

Typical TEM images for raw, sedimented and fractionated samples are shown in Fig. 8; obviously, the fractionation scheme resulted in the gradual elimination of large particles, allowing observation of submicron particles. This is in qualitative agreement with the PCS results of Fig. 10.

However, contrary to PCS, medium resolution TEM showed many particles smaller than 100 nm, down to a few nanometers in size, both in centrifugates [Fig. 8(c) and 8(d)] and in filtrates [Fig. 8(f) and 8(g)]. In addition, high resolution TEM (Fig. 11) showed that all samples contained many "large" (50–300 nm) organic fibrils, filaments or spongy networks. It must be noted that special techniques are required in order to visualize these organic matrices, due to their low electron density. Careful observations of TEM pictures under high contrast conditions suggested frequent associations of small inorganic colloids with the (often much) larger organic matrices (Fig. 11).

Therefore, all of the TEM observations made during this study suggested that a large fraction of the inorganic microcolloids (<50 nm) was associated with larger organic matrices. Such an association could also explain several other results:

- Association of microcolloids with larger organic matrices could explain the fact that no particle smaller than 50–100 nm was observed by PCS, despite its obvious existence (although the low sensitivity of PCS for these very small particles might also be a limitation). Since organic matrices of 200–300 nm were not removed from suspension by the centrifugation conditions used (see above), microcolloids associated with these organic matrices would also remain suspended. After centrifugation, PCS would measure only the size of the organic matrices.
- The much lower concentrations of microcolloids smaller than 50 nm in the filtrate of 0.05 μm membrane filtrations compared to that of 0.8 μm membrane filtrations [Fig. 8(f) and 8(g)] might also be explained by the association of microcolloids with larger organic matrices. Microcolloids smaller than 50 nm associated with organic matrices of 200–300 nm may have passed through 0.8 μm membranes, but were retained by 0.05 μm membranes.
- Coagulation models for hydrophobic colloids (Newman *et al.*, 1994) predict that the concentration of hydrophobic microcolloids in water should be below practical detection limits of TEM (the concentration of 10 nm particles left unaggregated after 2 days should be less than 10^{-24} mg/l for an initial concentration of 1 mg/l of particles with a uniform distribution in the range 1–100 nm). However, colloidal particles of a few nanometers were visible by TEM (Fig. 8); these small colloids may appear as isolated entities under low contrast TEM, while they are in reality bound to thin hydrophilic organic filamentous material, which are not considered in classical coagulation models. These associations have been observed in this work and in others (Pizarro *et al.*, 1994).
- Finally, the values of electrophoretic mobility also suggest that measured signals were dominated by the behavior of organic compounds.

In summary, the combination of results from different analytical techniques (LS, PCS, TEM,

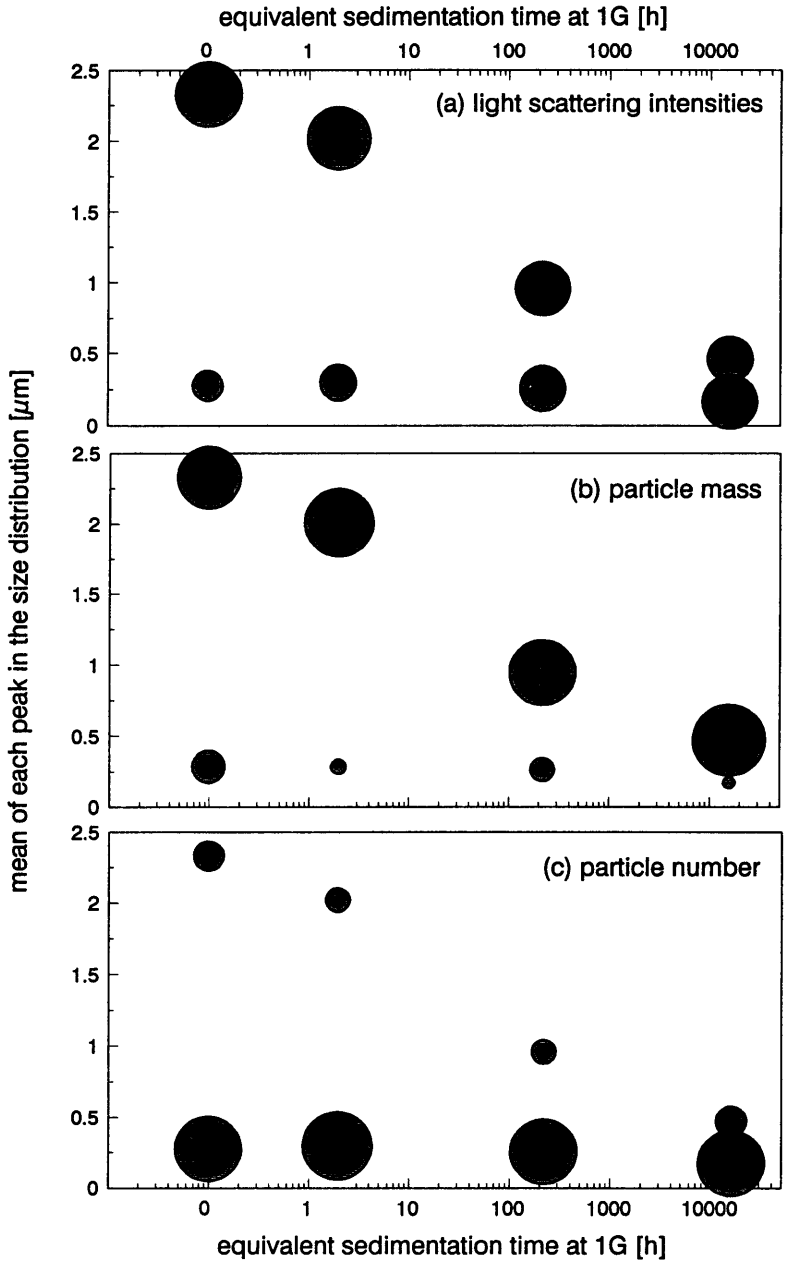

Fig. 10. PCS results of raw, sedimented and centrifuged Rhine River samples, expressed in (a) light scattering intensities, (b) particle mass (proportional to particle volume weighed distribution) and (c) particle number. Centrifugation times have been converted to equivalent sedimentation times at 1 ***g***. For each equivalent time, surfaces of circles represent the proportion of particles of the considered size. Variabilities on these proportions are 10–15% for (a) and (b) and *c.* 50% for (c) (see text). Sampling date: 22 October 1991.

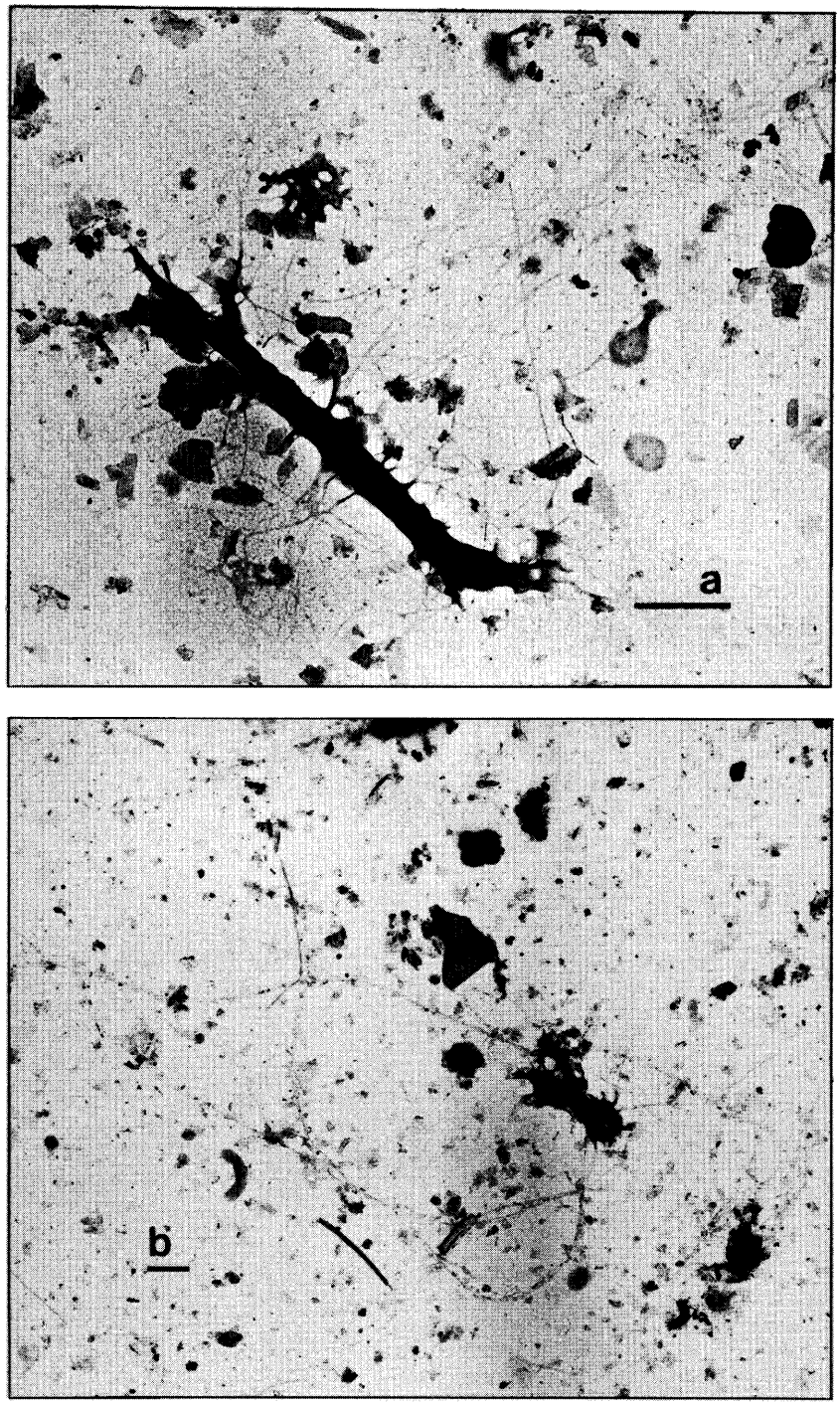

Fig. 11. High resolution/high contrast TEM showing the typical associations between organic fibrils or networks and inorganic particles of sizes smaller than 50 nm. Bar = 0.5 μm. Sampling date: 6 November 1990.

Table 3. Distributions of particle mass, number and specific surface area for the entire 1990–1991 Rhine River campaign; the method of estimating masses is discussed in Newman *et al.* (1994)

Size class (nm)	<200	200–700	700–1000	1000–3000	>3000
% of total mass	1.5 ± 1.1	9.5 ± 4.0	3.7 ± 3.9	26.2 ± 22.0	59.1 ± 24.1
Average size (nm)	100	450	850	2000	5000
% of total number	92.9 ± 68.2	6.5 ± 2.7	0.38 ± 0.4	0.20 ± 0.17	0.03 ± 0.01
% of total specific surface area	23.0 ± 16.9	32.4 ± 13.6	6.8 ± 7.2	19.9 ± 16.7	18.0 ± 7.3
Average size (nm)	30	450	850	2000	5000
% of total number	99.8 ± 73.2	0.19 ± 0.08	0.01 ± 0.01	<0.01	<0.01
% of total specific surface area	49.6 ± 36.3	21.3 ± 9.0	4.4 ± 4.6	13.1 ± 11.0	11.7 ± 4.8

Distributions of particle number and specific surface area have been estimated using two sets of average sizes for each given size class: $\bar{d} = 100$, 450, 850, 2000, 5000 nm and $\bar{d} = 30$, 450, 850, 2000, 5000 nm, with an average density of 2.0 g/cm^3. % of total particle number and specific surface area for particles smaller than 200 nm are certainly underestimated, considering that these particles are commonly non-rigid spheres with a porous surface structure.

ICP–AES, TOC) indicated that the majority of submicrometer inorganic particles were composed of clays, silica and iron oxyhydroxides, the sizes of which are sometimes as small as a few nanometers. Schematically, one can discriminate between:

- Inorganic particles larger than 1–3 μm, which constitute the largest proportion in mass, and which sediment quickly.
- Inorganic particles with sizes between 100 nm and 1 μm, which sediment slowly.
- Inorganic particles smaller than 100 nm, which are largely associated with, and stabilized by, organic matrices.

These latter associations appear in the form of organic fibrils (usual size: 0.1–1 μm) or sponge-like unfolded networks, at the surface and in the bulk of which inorganic entities with sizes smaller than 50 nm are attached. It is suggested that association of microcolloids with these organic matrices may influence their stability in the water column; this is important, since microcolloids can also play an important role as scavengers. Indeed, although the mass concentration of particles smaller than 0.2 μm is less than 2% of the total mass of particles, they have a high specific surface area (see Table 3).

Part II of this series (Newman *et al.*, 1994) reports the temporal evolution of particle size distributions in the Rhine River based on the analytical scheme discussed here, and its comparison to predictions based on a classical coagulation/sedimentation model. This complete scheme may also be useful in other aquatic environments (lakes, groundwaters) without major modification.

Acknowledgements—The authors wish to thank Dr G. G. Leppard (Canada Center for Inland Waters, Burlington, Ontario) for his work on high resolution TEM, Dr Vollmer (Gewässerschutzamt Basel-Stadt) for his cooperation and help in the field and F. Bujard and C. Bernard (Department of Inorganic, Analytical and Applied Chemistry of the University of Geneva) for the conception of the sedimentation tanks and filtration cells. This work was supported by a grant from Sandoz S. A. (Fonds Sandoz en Faveur du Rhin).

REFERENCES

Anderson M. A. and Rubin A. J. (1981) *Adsorption of Inorganics at Solid–Liquid Interfaces*. Ann Arbor Science, Ann Arbor, Mich.

Baccini P. (1984) Regulation of trace metal concentrations in freshwater systems. In *Metal Ions in Biological Systems* (Edited by Siegel H.), Vol. 18, pp. 329–286. Dekker, New York.

Bryant R. and Williams D. J. A. (1987) The electrochemistry of colloidal particles from a proglacial lake. *Chem. Geol.* **62,** 291–305.

Buffle J. (1988) *Complexation Reactions in Aquatic Systems: An Analytical Approach*. Horwood, Chichester.

Buffle J. and Van Leeuwen H. P. (1992) *Foreword in Environmental Particles I* (Edited by Buffle J. and Van Leeuwen H. P.). Lewis, Chelsea, Mich.

Buffle J., Perret D. and Newman M. (1992) The use of filtration and ultrafiltration for size fractionation of aquatic particles, colloids and macromolecules. In *Environmental Particles I* (Edited by Buffle J. and Van Leeuwen H. P.), pp. 171–230. Lewis, Chelsea, Mich.

Burdon K. L. and Williams R. P. (1969) *Microbiology*, 16th edition. Macmillan, New York.

Cresser M., Ebdon L., Armstrong J., Dean J., Ramsey M. H. and Cave M. (1990) Atomic spectrometry update—environmental analysis. *J. analyt. atom. Spectromet.* **5,** 1R–55R.

EAWAG (1989) Provisorische Zusammenstellung der Ergebnisse chemischer Analysen in Wochensammelproben ausgewählter Flüsse 1988; Messungen im Rahmen des nationalen Programms für die analytische Daueruntersuchung schweizerischer Fliessgewässer (NADUF).

Ford N. C. (1983) The theory and practice of correlation spectroscopy. In *Measurement of Suspended Particles by Quasi-elastic Light Scattering* (Edited by Danke B. E.), pp. 31–77. Wiley, New York.

Foulkes M. E., Ebdon L. and Hill S. (1988) Ore and mineral analysis by slurry atomisation–plasma emission spectrometry. *Analyt. Proc.* **25,** 92–94.

Fox L. E. (1988) The solubility of colloidal ferric hydroxide and its relevance to iron concentration in river water. *Geochim. cosmochim. Acta* **52,** 771–777.

Frösch D. and Westphal C. (1989) Melamine resins and their application in electron microscopy. *Electron. Microsc. Rev.* **2,** 231–255.

Gaigalas A. K., Woo S. and Hubbard J. B. (1990) The electrophoretic response of submicron particles to alternating electric fields. *J. Colloid Interface Sci.* **136,** 213–223.

Gallegos C. L. and Menzel R. G. (1987) Submicron size distribution of inorganic suspended solids in turbid waters by photon correlation spectroscopy. *Wat. Resour. Res.* **23,** 596–602.

Harfield J. G. and Bunker R. C. (1988) Measuring zeta potential and electrophoretic mobility by laser doppler velocimetry. *Filtrn Sepn* **Nov/Dec,** 412–415.

Kavanaugh M. C. and Leckie J. O. (1980) Particulates in water. In *Advances in Chemistry Series*, Vol. 189. American Chemical Society, Washington, D.C.

Leppard G. G. (1992) Evaluation of electron microscopic techniques for the description of aquatic colloids. In *Environmental Particles I* (Edited by Buffle J. and Van Leeuwen H. P.), pp. 231–289. Lewis, Chelsea, Mich.

Lerman A. (1979) *Geochemical Processes*. Wiley–Interscience, New York.

Newman M. E. and Buffle J. (1994) Capabilities of photon correlation spectroscopy for determining size distributions of submicron colloids in natural waters. In preparation.

Newman M. E., Filella M., Chen Y., Négre J.-C., Perret D. and Buffle J. (1994) Submicron particles in the Rhine River—II. Comparison of field observations and model predictions. *Wat. Res.* **28,** 107–118.

Nomizu T., Nozue T. and Mizuike A. (1987) Electron microscopy of submicron particles: morphology and elemental analysis of particles in fresh waters. *Mikrochim. Acta* **II,** 99–106.

Perret D., Leppard G. G., Müller M., Belzile N., De Vitre R. and Buffle J. (1991) Electron microscopy of aquatic colloids: non-perturbing preparation of specimens in the field. *Wat. Res.* **25,** 1333–1343.

Pizarro J., Belzile N., Filella M., Leppard G. G., Perret D. and Buffle J. (1994) Factors affecting coagulation/sedimentation of lake-born iron oxyhydroxide particles. Submitted to *Wat. Res.*

Rees T. F. and Ranville J. F. (1988) Characterization of colloids in the Mississippi river and its major tributaries. U.S. Geological Survey Toxic Substances Hydrology Program. In *Proceedings of the Technical Meeting, Phoenix, Arizona, 26–30 Sept.* (Edited by Mallard G. W. and Ragone S. E.), Water Resources Investigation Report 88, p. 4220.

Rees T. F. and Ranville J. F. (1990) Collection and analysis of colloidal particles transported in the Mississippi River, USA. *J. contam. Hydrol.* **6,** 241–250.

Salim R.and Cooksey B. G. (1981) The effect of centrifugation on the suspended particles of river waters. *Wat. Res.* **15,** 835–839.

Salomons W. and Förstner U. (1984) *Metals in the Hydrocycle*. Springer, Berlin.

Schurtenberger P. and Newman M. (1993) Characterization of biological and environmental samples using static and dynamic light scattering. In *Environmental Particles II* (Edited by Van Leeuwen H. P. and Buffle J.). Lewis, Chelsea, Mich.

Sigg L. (1987) Surface chemical aspects of the distribution and fate of metal ions in lakes. In *Aquatic Surface Chemistry* (Edited by Stumm W.), pp. 319–349. Wiley–Interscience, New York.

Stumm W. (1985) *Chemical Processes in Lakes*. Wiley–Interscience, New York.

Stumm W. (1987) *Aquatic Surface Chemistry*. Wiley–Interscience, New York.

Tipping E. and Higgins D. C. (1982) The effect of adsorbed humic substances on the colloid stability of hematite particles. *Colloid. Surf.* **5,** 85–92.

Van de Meent D., Los A., Leeuw J. W., Schen P. A. and Haverkamp J. (1983) Size fractionation and analytical pyrolysis of suspended particles from the River Rhine delta. In *Adv. Organ. Geochem. 1981* (Edited by Bjorøy M. *et al.*), pp. 336–349. Wiley, Chichester.

Wells M. L. and Goldberg E. D. (1991) Occurence of small colloids in sea water. *Nature* **353,** 342–344.